AD-A064 246 COMMUNICATIONS RESEARCH CENTRE OTTAWA (ONTARIO) F/G 14/5
OPTICAL-RECORDER DESIGN CONSIDERATIONS FOR THE CANADIAN SEASAT --ETC(U)
NOV 78 E B FELSTEAD, G E HASLAM

UNCLASSIFIED CRC-TN-695 NL

1 OF 1
ADA
064246

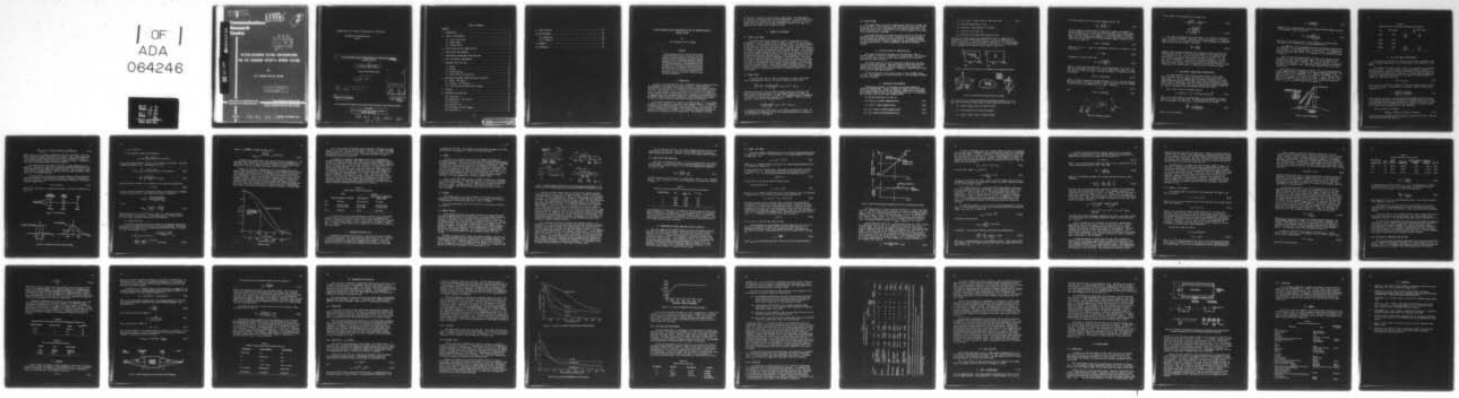

END
DATE
FILMED
4-79
DDC

LEVEL II

3
B.S.

Communications Research Centre

OPTICAL-RECORDER DESIGN CONSIDERATIONS FOR THE CANADIAN SEASAT-A GROUND STATION

by

E.B. Felstead and G.E. Haslam

DEPARTMENT OF COMMUNICATIONS
MINISTÈRE DES COMMUNICATIONS

CRC TECHNICAL NOTE NO. 695

This work was sponsored by the Department of National Defence, Research and Development Branch under Project No. 33D16.

CANADA

79 01 29 080

OTTAWA, NOVEMBER 1978

COMMUNICATIONS RESEARCH CENTRE

DEPARTMENT OF COMMUNICATIONS
CANADA

(6) # OPTICAL-RECORDER DESIGN CONSIDERATIONS FOR THE CANADIAN SEASAT-A GROUND STATION .

by

(10) E.B/Felstead and G.E/Haslam

(Radio and Radar Research Branch)

(12) 40p.

(14) CRC-TN-695

(9) TECHNICAL NOTE

(11) November 1978

OTTAWA

This work was sponsored by the Department of National Defence, Research and Development Branch under Project No. 33D16.

TABLE OF CONTENTS

OPTICAL-RECORDER DESIGN CONSIDERATIONS FOR THE CANADIAN SEASAT-A GROUND STATION

by

E.B. Felstead and G.E. Haslam

ABSTRACT

A synthetic-aperture radar will be one of the major instruments on board the SEASAT-A satellite. A recorder is to be built and installed at the Canadian ground station. Its purpose is to record the received signals as an interferogram appropriate for subsequent processing. In this note, system design considerations are given. The 19 MHz bandwidth signal is to be recorded with 2 CRT's each covering half of the 100 km swath. Two drives move film past the CRT. Specification of CRT velocity and linearity and film velocity and stability are given. The modulation transfer function required for the CRT, lens and film are given. Exposure levels are calculated and compared to sensitivities of certain films. A table summarizes the specifications.

1. INTRODUCTION

As part of the Canadian effort for the SEASAT-A remote sensing satellite, the Department of National Defence (DND), through the Defence Research Establishment Ottawa (DREO), has undertaken the task of developing an optical recorder. This recorder is to be installed at the Canadian ground station in Shoe Cove, Newfoundland, where its purpose will be to store the synthetic-aperture radar's signal on photographic film. The format of the storage will be appropriate for the subsequent production of imagery using coherent-optical processing. DREO has also been assigned the task of developing the system, (called an optical correlator) which does this optical processing.

This report represents the results of a study carried out at the request of DREO and in collaboration with their Remote Sensing Section. It presents a preliminary specification and design for the recorder. It does *not* cover any of the subsequent detailed design, construction, testing and calibration. In Section 2, the nature of the signal to be recorded is described, followed in Section 3 by a description of CRT capabilities. The subsequent sections,

(a) describe an attempt to match recorder capabilities to the SAR signal, (b) consider problem areas and (c) give specifications. The operation of the recorder and the correlator are very interdependent. Therefore, in order to ensure that one system does not make unrealistic demands on the other, the design of both systems is an iterative process.

2. SIGNAL TO BE RECORDED

2.1 FORM OF THE SIGNAL

The SEASAT-A SAR system transmits a series of pulses where (a) the pulsewidth, τ, is 33.8 μs and (b) the frequency of the carrier for the pulse is chirped, or varied linearly with time, through 19 MHz. The pulses received by the radar, as a result of reflection from the terrain, are mixed down in frequency so that they occupy the band between 2 MHz and 21 MHz. The bandwidth is 19 MHz, the same as the bandwidth of the transmitted pulse. This signal is then used to intensity-modulate the electron beam of a cathode ray tube, (CRT). The electron beam of the CRT is swept, on a line, across the face of the CRT, in synchronism with the returning pulses. A film is moved across the face of the CRT, in a direction which is transverse to the above lines. The format of the data stored on the film is therefore a series of successive lines down the length of the film where each line runs across the film. Position along a line can be associated with slant range. We will therefore call the along-line data the range signal. The position defined by moving from line to line, along the length of the film, is associated with the azimuth dimension. The azimuth signal is a sampled function where the sampling frequency is the PRF of the radar.

2.2 RANGE SIGNAL

The ground range swath of 100 km corresponds to a slant range swath, Δr_s, of approximately 38.4 km. The time to record the width Δr_s is

$$\frac{2\Delta r_s}{c} + \frac{2\tau}{2} = \frac{2 \times 38.4 \times 10^3}{3 \times 10^8} + 33.8 \times 10^{-6} = 290\ \mu s.$$

The extra width $2\tau/2 = 33.8$ μs arises from the overlap at each end of the swath of the uncompressed pulse. At the maximum frequency of 21 MHz, the total number of cycles is $290 \times 21 = 6090$. If recording is made in subswaths, the same 33.8 μs overlap must be added to each subswath. Thus, if two subswaths are used, then the recording time is

$$\frac{2 \times 38.4 \times 10^3}{2 \times 3 \times 10^8} + 33.8 \times 10^{-6} = 161.8\ \mu s$$

per subswath which gives 3398 cycles of the highest frequency of 21 MHz. For four subswaths the recording time is 97.8 μs per subswath which corresponds to 2054 cycles of 21 MHz signal.

2.3 AZIMUTH SIGNAL

The azimuth signal is written as samples along the film at the PRF rate. One of four PRF's, of approximately 1463.8, 1539.8, 1580.9 and 1646.8 Hz, may be selected for one pass. The highest one will likely be always used. The PRF is f_o/N where N is an integer and f_o is the centre frequency of the range offset, approximately 11.3824 MHz.

The azimuth bandwidth to be recorded is about 1040 Hz so that even the minimum PRF obeys the sampling theorem. However pitch, yaw and equivalent yaw can displace the spectrum by as much as 1850 Hz. The sampling theorem can still be applied but requires the samples to be recorded very accurately in their proper position. Precise triggering of the CRT is therefore required.

3. STATE-OF-THE-ART CRT CHARACTERISTICS

Many types of phosphor are available for CRT recording. The P11 phosphor appears to be the most suitable for the task at hand. This phosphor has a spectral peak at 460 nm, a decay time to 10% of 35 μs, and can be produced with a very fine grain.

The highest resolution in CRT's is achieved utilizing very high beam voltages and low beam currents. High beam voltages reduce electron transit time and hence beam spreading. Thirty kV appears to be the upper limit imposed by X-ray radiation considerations. Typically, a beam current of about 1 μa is used for high resolution work.

The state-of-the-art in spot size is about 6.5 mils (0.00065 inches, 16.5 μm). This resolution can be maintained over a 4.25 inch sweep if dynamic focussing is employed.

4. ASPECT-RATIO RELATIONSHIPS

As mentioned previously, the recorder and correlator design are critically interdependent. Here, we consider the aspect ratio of the signal and of the correlator and how they are combined. Aspect ratio is the ratio of the azimuth dimension scale to the range dimension scale. It is desirable that the aspect ratio of the output image be unity.

For the CRT recording on to film, let

$$p = (V/c_a)/v_f = \text{azimuth demagnification}, \tag{4.1}$$

$$q = c/(2v_c) = \text{range demagnification}, \tag{4.2}$$

$$m_a = 1/p = \text{azimuth recording magnification}, \tag{4.3}$$

$$m_r = 1/q = \text{range recording magnification}, \tag{4.4}$$

$A_f = q/p = m_a/m_r$ = aspect ratio of input data film, (4.5)

c_a = velocity scale factor = 1.13,

V = velocity of the satellite = 7.64 km/s,

v_f = velocity of the film, and

v_c = velocity of the light beam across the film.

Note that A_f is the aspect ratio K described in [1]. A signal that is recorded as a (1/p) x (1/q) square for $A_f = 1$, would be recorded, as in Figure 4.1(a) for $A_f > 1$ and as in Figure 4.1(b) for $A_f < 1$. The coordinate x_f is the azimuth dimension recorded on the film and r_f is the range dimension. Consider now the optical system shown in Figure 4.2.

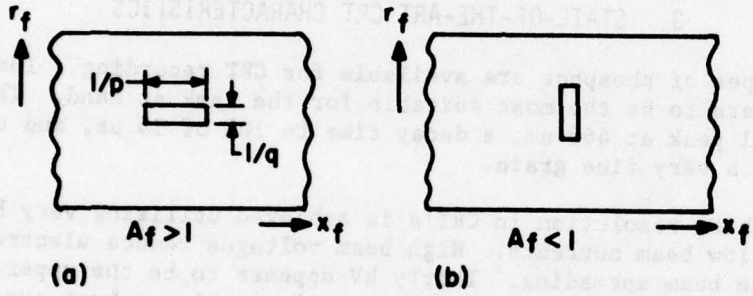

Figure 4.1. Dimensions of a Unit Square on the Interferogram for Two Different Aspect Ratios

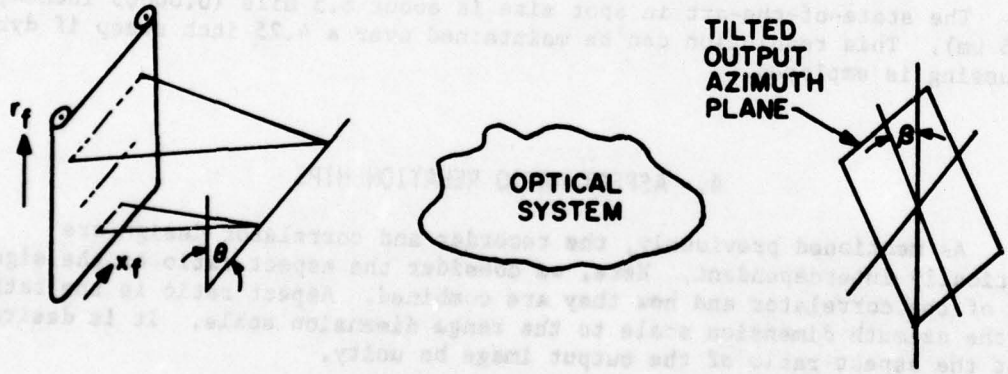

Figure 4.2. Input and Output Tilts When Input Film is Not Tilted

It is based on the tilted-plane processor described by Kozma et al. [1]. Only the tilted output azimuth plane is shown (range plane omitted). Let

M_a = azimuth magnification of optical system

M_r = range magnification of optical system

$A_o = M_a/M_r$ = aspect ratio of optical system.

For unity aspect ratio of the output image we require that

$$A_f A_o = \frac{m_a}{m_r}\frac{M_a}{M_r} = 1. \tag{4.6}$$

The tilt angles of various planes in the optical system are dependent on various parameters of the radar and on both the aspect ratio of the signal and the optical system. It is important to keep these angles relatively small. For the tilted-plane processor, it can be shown that for a vertical input film the tilt angle β of the output azimuth image is related to the tilt θ of the input by

$$\tan\beta = -(\tan\theta)A_o^2. \tag{4.7}$$

Therefore, for $A_o < 1$, there is a substantial reduction in the angle β. Note that usually

$$\beta \simeq -\theta A_o^2. \tag{4.8}$$

Furthermore, it may be shown that

$$\beta = \tan^{-1}\left|\frac{\lambda_r A_f A_o^2}{2p\lambda_1}\right|. \tag{4.9}$$

where λ_r is the radar wavelength and λ_1 is the wavelength of the light. To make the range image plane fall on the tilted azimuth-image plane, the input film must be tilted by an angle α as shown in Figure 4.3. Equation (4.7) may be rewritten

$$\tan\alpha' = -\tan(\theta+\alpha)A_o^2, \tag{4.10}$$

where α is the tilt angle of the input film and $\alpha' = \beta+\varepsilon$ is the tilt angle of the output plane. The range telescope of this correlator is usually arranged so that there is unity magnification in range. Therefore

$$\alpha' = -\alpha \tag{4.11}$$

and

$$-\tan\alpha = -\tan(\theta+\alpha)A_o^2. \tag{4.12}$$

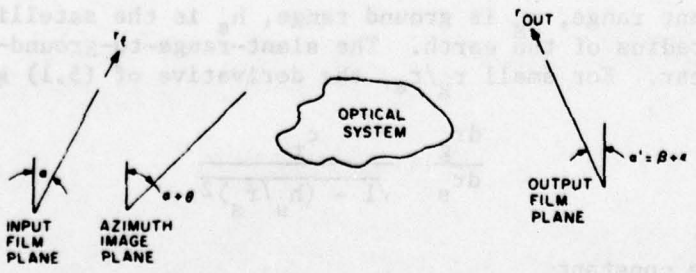

Figure 4.3. Tilt Angles for Correlator

If the tangent is approximated by the angle, then

$$\alpha = \frac{-\beta/A_o^2}{1/A_o^2 - 1} = \frac{-\beta}{1 - A_o^2} = -\alpha' \tag{4.13}$$

$$= \frac{-\tan^{-1}\left[\dfrac{\lambda_r A_f A_o^2}{2p\lambda_1}\right]}{1 - A_o^2} . \tag{4.14}$$

For practical operation of the correlator, it is desired to keep the tilt α as small as possible. Therefore, on the radar itself, it is useful to keep λ_r and $A_f/p = q/p^2$ as small as possible. The wavelength λ_r is fixed for SEASAT-A and cannot be altered. The factor

$$\frac{q}{p^2} = \frac{cV^2}{2v_c v_f^2} \tag{4.15}$$

depends on the recorder parameters and is therefore useful to contract the azimuth signal relative to the range with emphasis on the azimuth because p is squared in (4.15). For the correlator itself, it is seen that α is proportional to A_o squared and therefore is useful to make $A_o << 1$. For $A_o < 1$, the denominator $1 - A_o^2$ in (4.14) varies little with A_o. Since we want $A_f A_o = 1$, A_f and A_o cannot both be made small simultaneously in the factor $(A_f/p)A_o^2$. However, p can be made large (contracting in azimuth) while keeping A_f at the desired value, by making q large (contracting range).

5. SLANT-RANGE, GROUND-RANGE CONSIDERATIONS

The range dimension of the recorded signal refers to slant range. Also, the aspect ratios A_f and A_o are usually calculated with respect to slant range. If, for the SEASAT-A SAR, the image is presented in the slant range coordinates and with unity aspect ratio, then an extreme tilt in the output plane is experienced. The tilt could be reduced by reducing $(A_f/p)A_o^2$. In this section, it is shown that the tilt problem can be greatly reduced if the output is presented in an approximated ground-range format.

Slant range is related to ground range by

$$r_s = \left\{(h_s+r_e)^2 + r_e^2 - 2r_e(h_s+r_e)\cos(r_g/r_e)\right\}^{\frac{1}{2}} \tag{5.1}$$

where r_s is slant range, r_g is ground range, h_s is the satellite altitude, and r_e is the radius of the earth. The slant-range-to-ground-range conversion is nonlinear. For small r_g/r_e, the derivative of (5.1) gives

$$\frac{dr_g}{dr_s} \simeq \frac{c_r}{\sqrt{1 - (h_s/r_s)^2}} \tag{5.2}$$

where c_r is the constant

$$c_r = \frac{1}{\sqrt{1 + h_s/r_e}} . \tag{5.3}$$

Therefore, over a limited swath, the slant-range-to-ground-range conversion is approximately linear and given by

$$\Delta r_g = \frac{c_r \Delta r_s}{\sqrt{1 - (h_s/r_{sav})^2}} \tag{5.4}$$

where r_{sav} is the average value of slant range over the limited swath. Optically, this is implemented as a simple magnification.

For SEASAT-A, it was recommended that the processing be divided into five subswaths. This recommendation was based on worst case considerations on correcting for range curvature and 6.5 m resolution. Four subswaths are sufficient for most applications. The geometry for four subswaths is shown in Figure 5.1.

Table 5.1 shows the magnification in range, $M_{rc} = dr_g/dr_s$, for the conversion of slant range into ground range. It is calculated for the average slant range of each subswath. Also given is the error ε in M_{rc} at the edge of the subswath. It is seen that the worst magnification error at the edge of one subswath is 5%. Even between subswaths there is not much change in M_{rc}.

The reason that the nonlinear conversion (5.1) can be approximated by a simple magnification for SEASAT-A can be seen in magnification (5.2). The factor $(1-(h_s/r_s)^2)^{-\frac{1}{2}}$ is dependent on r_s. However, for SEASAT, r_s has a maximum spread of about ±19 km about an average r_s of about 860 km. Therefore, the r_s dependent factor varies very little. Compare this case to the airborne case where the magnification will vary considerably because the spread in r_s is of the same order as the average r_s.

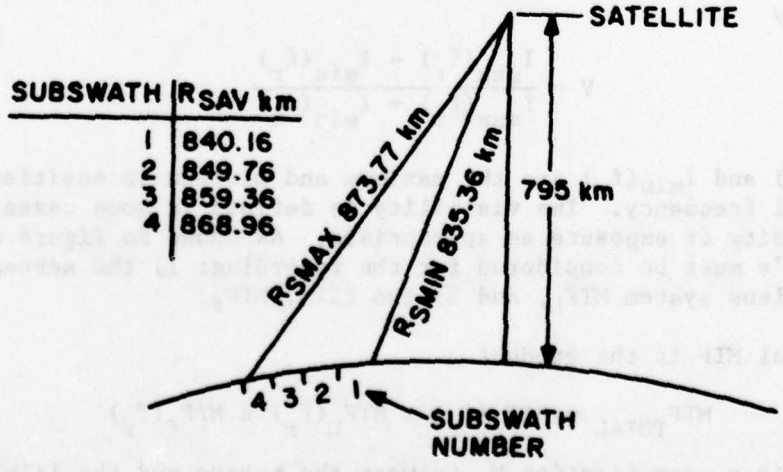

Figure 5.1. Division into Subswaths

TABLE 5.1

Magnification Required for Conversion of Slant Range to Ground Range

r_{sav}	$M_{rc} = dr_g/dr_s$	ϵ	$\frac{\epsilon}{M_{rc}} \times 100 = \%$ Error
840.16	2.916	+0.155	+5.3
		−0.132	−4.5
849.76	2.670		
859.36	2.483		
868.96	2.336	+0.070	+3.0
		−0.063	−2.7

6. SPOT SIZE AND MTF REQUIREMENTS

In this section, MTF and its relation to spot size is discussed. The spatial frequency requirements of the three stages of the recorder are then given.

The modulation transfer function (MTF) is the amplitude of the optical transfer function. The MTF describes the spatial-frequency response of incoherent optical systems and therefore is defined in terms of intensities. If a sinusoidal fringe pattern is the input to a linear optical system, the output is a sinusoidal fringe pattern, but usually of reduced contrast or visibility. Here we use the form

$$MTF = V_{out}/V_{in} \tag{6.1}$$

where V_{in} is the visibility (contrast) of the input signal and V_{out} is that of the output signal. The visibility is defined in terms of power density (intensity) by

$$V = \frac{I_{max}(f_r) - I_{min}(f_r)}{I_{max}(f_r) + I_{min}(f_r)} \tag{6.2}$$

where $I_{max}(f_r)$ and $I_{min}(f_r)$ are the maximum and minimum intensities and f_r is the spatial frequency. The visibility is defined in some cases in terms of energy density or exposure as appropriate. As shown in Figure 6.1, three different MTF's must be considered for the recording: 1) the screen, MTF_s, 2) the relay lens system MTF_L, and 3) the film, MTF_f.

The total MTF is the product

$$MTF_{TOTAL} = MTF_s(f_r) \times MTF_L(f_r) \times MTF_f(f_r) \tag{6.3}$$

Often, there is a magnification M_L between the screen and the film. Then the total MTF recorded on the film is

$$MTF_{TOTAL}(f_r) = MTF_s(f_r/M_L)MTF_{LO}(f_r/M_L)MTF_f(f_r) \quad (6.4)$$

where, now, f_r is the spatial frequency *at the film*, and MTF_{LO} is the lens MTF in terms of spatial frequencies at the object. MTF_s is discussed below. MTF_f and MTF_L are examined in Sections 8.1 and 9.1 respectively. MTF_s is not usually provided. Instead spot size is generally quoted. Therefore, we derive relations between MTF_s and spot size below.

Spot size refers to the width of the spot of light generated by the phosphor. Studies have shown that the spatial intensity distribution of the light emitted from the phosphor is usually Gaussian. The spot size is taken as the width "d" between the 1/2 intensity points as shown in Figure 6.2(b) where r_f is the spatial variable.

To find the MTF_s, we note that the electron beam is swept continuously across the phosphor. A sinusoidal test signal of frequency f Z-modulates the beam so that the electron current and therefore the power of the emitted light is proportional to

$$B + b \cos 2\pi ft \quad (6.5)$$

where B is a bias and b is a modulation constant. The input "visibility" is $V_{in} = b/B$.

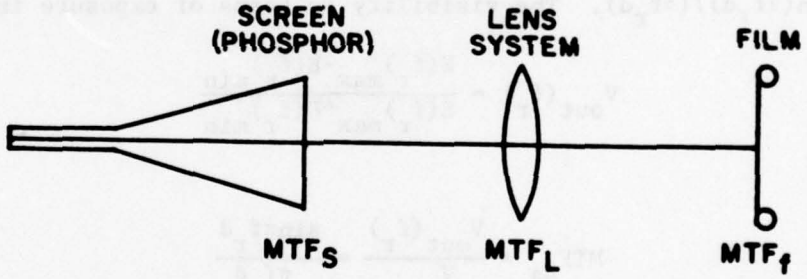

Figure 6.1. MTF's for Recorder

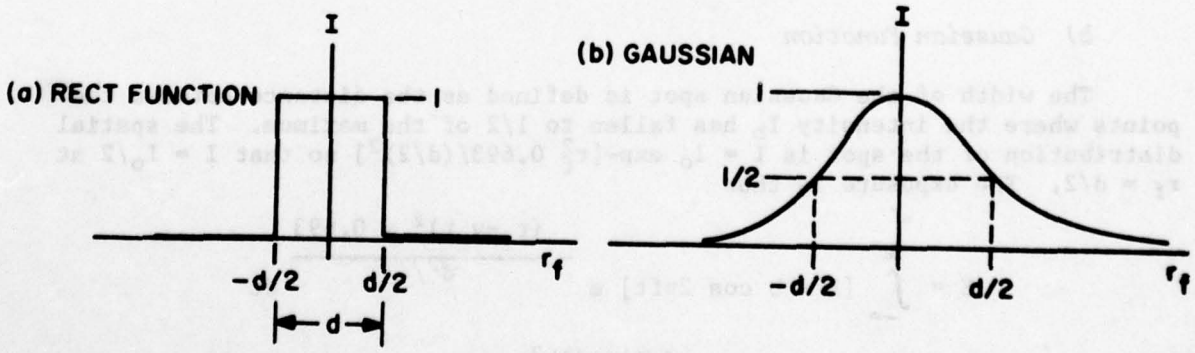

Figure 6.2. Two Models of Spot Shape of Light at Phosphor

a) Rect Function

At any instant of time the intensity is

$$I_a = \text{rect}\left[\frac{r_f - v_c t}{d}\right][B + b\cos 2\pi ft]$$

for the rect function model. Here v_c is the velocity of the spot. The time-integrated intensity, i.e., the exposure $E = It$ is

$$E(f_r) = \int_{-\infty}^{\infty} \text{rect}\left[\frac{r_f - v_c t}{d}\right][B + b\cos 2\pi ft]\,dt \qquad (6.6)$$

$$= \frac{Bd}{v_c} + \frac{bd}{v_c}\frac{\sin \pi f_r d}{\pi f_r d}\cos 2\pi f_r r_f, \qquad (6.7)$$

where the spatial frequency f_r is related to the input time frequency by

$$f_r = f/v_c \qquad (6.8)$$

In (6.7), we see the desired cosinusoidal signal is attenuated by a weighting function $\sin(\pi f_r d)/(\pi f_r d)$. The visibility in terms of exposure is

$$V_{out}(f_r) = \frac{E(f_r)_{max} - E(f_r)_{min}}{E(f_r)_{max} + E(f_r)_{min}}$$

so that

$$MTF_{sa} = \frac{V_{out}(f_r)}{V_{in}} = \frac{\sin \pi f_r d}{\pi f_r d} \qquad (6.9)$$

which is unity at $f_r = 0$ and is 0 at $f_r = 1/d$ (i.e., where pulse width d equals one cycle of sine wave). Interestingly, there is response beyond $f_r = 1/d$, albeit reversed in phase and of low amplitude.

b) Gaussian Function

The width of the Gaussian spot is defined as the distance between the points where the intensity I_b has fallen to 1/2 of the maximum. The spatial distribution of the spot is $I = I_o \exp-[r_f^2\ 0.693/(d/2)^2]$ so that $I = I_o/2$ at $r_f = d/2$. The exposure is thus

$$E = \int_{-\infty}^{\infty} [B + b\cos 2\pi ft]\, e^{-\frac{(r_f - v_c t)^2 \times 0.693}{d^2/4}}\,dt$$

$$= \frac{Bd'\sqrt{\pi}}{2v_c} + \frac{bd'\sqrt{\pi}}{2v_c} e^{-(\pi d' f_r/2)^2} \cos 2\pi f_r r_f \qquad (6.10)$$

where $d' = d/\sqrt{0.693}$. The MTF is found to be

$$MTF_{sb} = e^{-\left[\frac{\pi d' f_r}{2}\right]^2} := e^{-(1.89\ df_r)^2} . \qquad (6.11)$$

The MTF_s for a Gaussian and a rect spot are plotted in Figure 6.3. The abscissa is the product $f_r d$. The spatial frequency can be determined for a given spot size. For a 0.65 mil (16.5 μm) spot size, the abscissa is also given as f_r. Notice that MTF_s has fallen to 41% at 30 ℓp/mm.

Caution is necessary in reading spot size from manufacturer's data sheets. Many will give spot size as measured by the shrinking raster method. This method is subjective, and on the average, gives a value of spot size that corresponds to a measure of the 70% level of intensity rather than the desired 50% level. Thus, a more optimistic (smaller) value of spot size is obtained. The best method is to use one of several forms of analyzer that actually measures the spot profile under the same conditions of current, sweep rate, etc., that the CRT is to be actually used. These techniques use one or two slits and a photodetector to obtain the profile. These profile measurements can be made with equipment presently available at CRC and DREO.

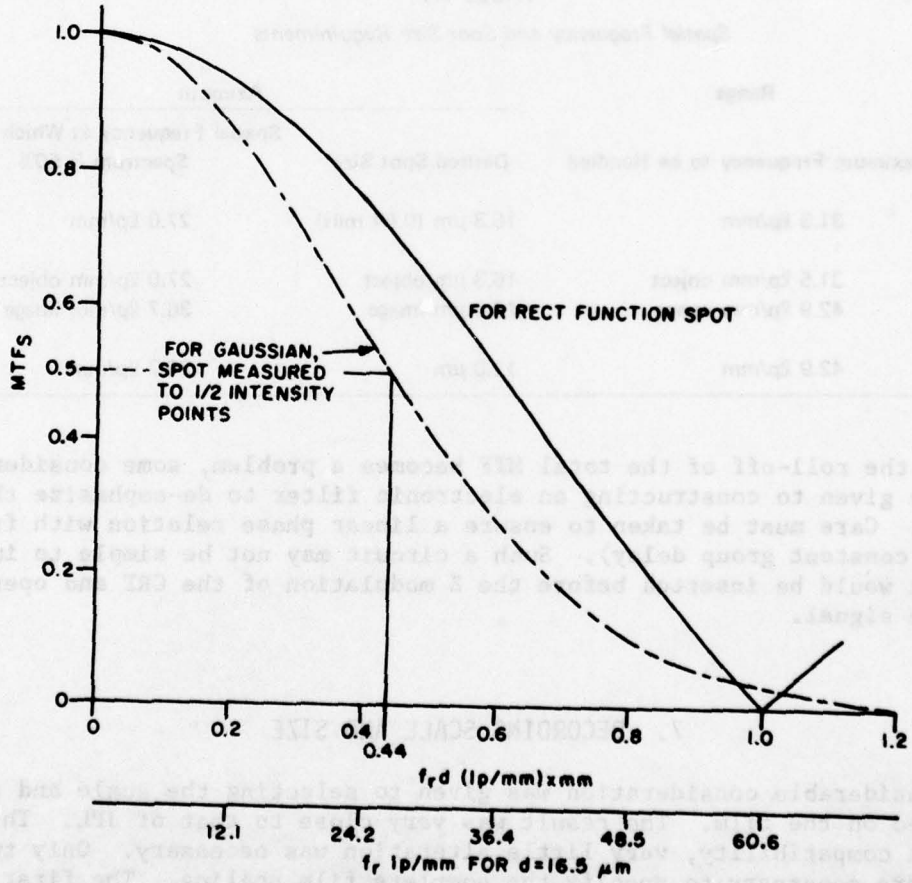

Figure 6.3. MTF's

Let us now consider the maximum spatial frequency or minimum spot size required at the CRT, through the lens, and at the film. In range the maximum spatial frequency at the film is 21 x $10^6/v_c$ = 42.9 ℓp/mm so that at the CRT the maximum is 42.9/1.36 = 31.5 ℓp/mm. The relay lens must be capable of relaying these spatial frequencies.

In azimuth, the frequency requirements are not so straightforward because the signal is sampled. Spot size is then a more meaningful measure but there is a problem in that film and lenses are usually rated in terms of spatial frequency only. As will be seen in Section 7.3, the highest PRF will result in a sample spacing of 24.3 μm at the film. In Section 7.3 it is further shown that the spot size at the film should be no more than 1/2 of the spacing so that a 12 μm spot is desired at the film. From Figure 6.3, it is seen that the power spectrum of a 12 μm spot has fallen to 50% at a spatial frequency of 0.44/(12x10^{-3}) = 36.7 ℓp/mm. Thus the film should possess a good MTF to at least 36.7 ℓp/mm. At the CRT a spot size of 12 x 1.36 = 16.3 μm (0.64 mils) is desired which corresponds to a fall in power spectrum of 50% at 27.0 ℓp/mm. Again the relay lens must be capable of transferring these spatial frequencies with little loss. The spot size and spatial frequency requirements are summarized in Table 6.1.

TABLE 6.1

Spatial Frequency and Spot Size Requirements

	Range	Azimuth	
	Maximum Frequency to be Handled	Desired Spot Size	Spatial Frequency at Which Power Spectrum is 50%
CRT	31.5 ℓp/mm	16.3 μm (0.64 mils)	27.0 ℓp/mm
LENS	31.5 ℓp/mm object 42.9 ℓp/mm image	16.3 μm object 12.0 μm image	27.0 ℓp/mm object 36.7 ℓp/mm image
FILM	42.9 ℓp/mm	12.0 μm	36.7 ℓp/mm

If the roll-off of the total MTF becomes a problem, some consideration should be given to constructing an electronic filter to de-emphasize the roll-off. Care must be taken to ensure a linear phase relation with frequency (i.e., a constant group delay). Such a circuit may not be simple to implement. It would be inserted before the Z modulation of the CRT and operate on the range signal.

7. RECORDING SCALE AND SIZE

Considerable consideration was given to selecting the scale and sizes to be used on the film. The result was very close to that of JPL. Therefore to obtain compatibility, very little alteration was necessary. Only two values were necessary to specify the complete film scaling. The first was the film velocity v_f = 40 mm/s and the second was the velocity of the beam

v_c measured *at the film*. JPL planned on putting 102 μs of signal in a 50 mm aperture which corresponds to a velocity of 4.90×10^5 mm/s.

7.1 RANGE

In Section 2.2, it was shown that as the number of subswaths is increased, the total number of cycles that must be recorded is also increased. As noted elsewhere, it is required to process over no less than four subswaths to ensure that range curvature correction is adequately performed. After consideration of the various trade-offs it was found that a good solution is to record two subswaths. Two CRT's are used to record onto two films. Each of the two subswaths will be capable of recording 161.8 μs of signal. To process over four subswaths, each film will be processed twice - one for the top half and once for the bottom. Because of overlap required between subswaths, it is not appropriate to slice the films in half.

At $v_c = 4.90 \times 10^5$ mm/s, 161.8 μs of signal is recorded in a distance of 79.3 mm (3.12 inches). A useful CRT width for the CRT's under consideration is 4.25 inches (108 mm). Thus the magnification required between CRT and film is 1.36:1 (a demagnification). The range scale factor is $q = c/(2\ v_c) = 306000$. The electron beam velocity v_b at the CRT is $1.36\ v_c = 6.66 \times 10^5$ mm/s.

7.2 AZIMUTH

The azimuth scale is $p = V/c_a v_f$) where V is the satellite velocity relative to a stationary earth and $c_a = 1.13$ is a constant. The velocity V is approximately 7.64 km/s near Shoe Cove. Thus, $p = 169027$.

For a ten minute pass, $40 \times 10^{-3} \times 60 \times 10 = 24$ m (79 feet) of film are required.

7.3 SAMPLE SPACING

In the azimuth direction, the signal is written in sampled form with the sample shape being that of the spot shape. The sample shape recorded on film can be different than the CRT beam spot shape because of film non-linearity, thresholding, and graininess. In many recorders to date, such as the ERIM dual-band [2] and the CRC modified APS-94D, the samples are recorded heavily overlapped. This overlap is permissible in both examples cited because the sample rate (the PRF) is much larger than the azimuth (doppler) bandwidth. However, for SEASAT-A, even the highest PRF is only slightly greater than the doppler bandwidth. It is shown below for SEASAT-A, that not only is overlap undesirable but even contiguous samples are to be avoided.

Consider a Gaussian spot of width w as shown in Figures 7.1(a) and (c). The peak of the Gaussian is that of the function at the sample instant. The azimuth signal a(t) is sampled at the PRF = f_p. Let the film velocity be v_{f1} for Figure 7.1(a). Then the signal shown in Figure 7.1(a) is $a'(x_f) = a(x_f/v_{f1})$ sampled at $X_1 = v_{f1}/f_p$ intervals. The spacing X_1 is chosen so that samples are touching (contiguous) in the sense that $X_1 = w$.

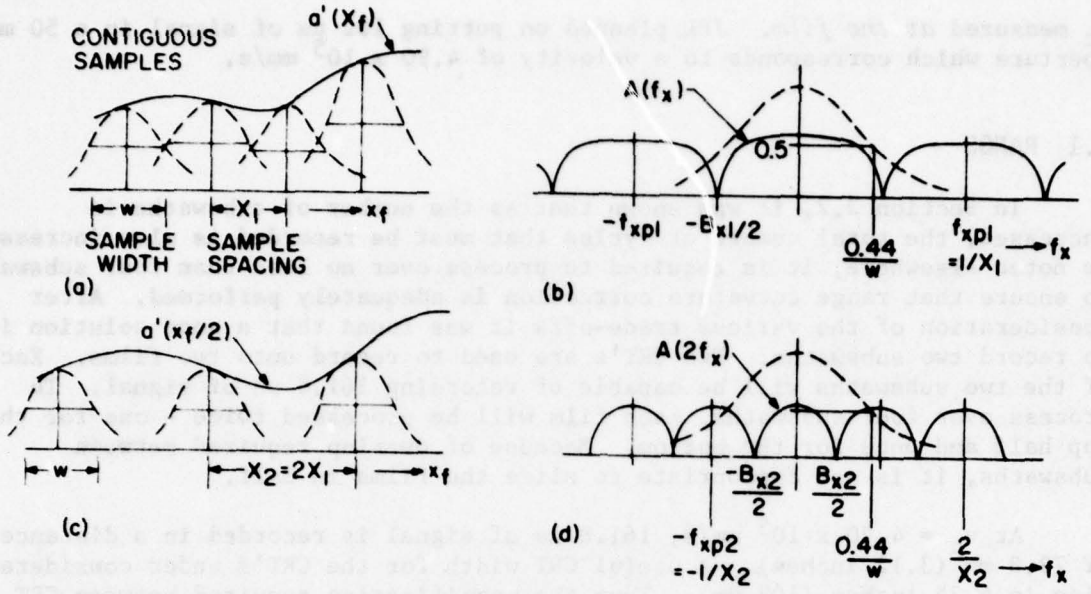

Figure 7.1. Sampled Time Signal and its Spectrum for (a) and (b) Contiguous Samples Recorded at a Film Velocity v_{f1} and (c) and (d) Sample Spacing Twice the Sample Width Recorded at a Film Velocity $v_{f2} = 2v_{f1}$.

Since the x_f domain signal does not directly show problems caused by sample spacing, we look now at the frequency domain. It may be shown that the spectrum has the form shown in Figure 7.1(b) where $A(f_x)$ is the transform of $a'(x_f)$. It has a bandwidth B_{x1}. Because of the sampling, the amplitude spectrum $A(f_x)$ is repeated at intervals of $f_{xp1} = 1/X_1$. For the illustration, $f_{xp} = B_x$. The repeated spectra have a weighting shown by the dashed line. This weighting, $\exp(-3.56\ w^2 f_x^2)$, is the Fourier transform of the individual sample shape. It is unity at $f_x = 0$, and is down to 0.5 at $f_x = 0.44/w$. Such a weighting would not be much of a problem, in fact may be useful for aperture tapering in azimuth, except for the presence of pitch and yaw. They cause the repeated spectra to shift in the f_x direction whereas the weighting remains fixed. For SEASAT-A, the expected maximum pitch and yaw could cause the desired 0 order spectrum $A(f_x)$ to shift at least its own bandwidth. The desired spectrum would be badly distorted. Furthermore, if it is desired to estimate the doppler centroid from the spectrum obtained optically, this estimation is made extremely difficult.

It is therefore necessary to broaden the weighting relative to the bandwidth B_x. To do this, the sample width must be made as small as possible relative to the sample spacing. For example suppose the film velocity is increased from v_{f1} to v_{f2} while the spot width remains constant. For $v_{f2} = 2v_{f1}$, the sample spacing X_2 is 2w as shown in Figure 7.1(c). In the frequency domain shown in Figure 7.1(d), the weighting is unaltered, but the repeated spectra are shrunk so that $B_{x2} = B_{x1}/2$. Furthermore, the PRF spacing is now $f_{xp2} = f_{xp1}/2$. For pitch and yaw sufficient to shift the spectrum an amount $\pm B_{x2}$, the resulting 0 order spectrum would be unsymmetrically weighted but it is probably tolerable. Unsymmetrical weighting would also mean that the doppler centroid estimation is made more difficult. It is preferable that the sample spacing should be at least twice the sample width.

If a 6.5 mil spot (16.5 μm) is actually obtained, the spot size at the film would be 16.5 μm/1.36 = 12.13 μm. At the highest PRF of 1647 Hz the sample spacing would be 40 x 10^3/1647 = 24.3 μm, the minimum desired spacing.

7.4 ASPECT-RATIO CONSIDERATIONS

From (4.6) we require that $A_f A_o = 1$ for unity aspect-ratio with respect to slant range. To incorporate the slant-range-to-ground-range conversions, the values of M_{rc} listed in Table 5.1 for the four subswaths are inserted into (4.6) so that

$$A_f A_o = \frac{m_a}{m_r}\frac{M_a}{M_r} = \frac{1}{M_{rc}} \tag{7.1}$$

for unity aspect ratio with respect to ground range. With $A_f = q/p = 306{,}000/169027 = 1.81$, the values of A_o for each subswath are calculated and tabulated in Table 7.1.

TABLE 7.1

Aspect Ratio of Optical System Required to Give Unity Aspect Ratio in Ground Range

Subswath Number	M_{rc}	$\frac{1}{A_f M_{rc}} = A_o$	$K' = 1/A_o$
1	2.916	0.190	5.28
2	2.670	0.207	4.83
3	2.483	0.223	4.49
4	2.336	0.237	4.23

Also tabulated is the value $K' = 1/A_o$ which is the often used "K" value of an optical correlator. For example, $K = 4$ is the nominal value for the present DREO correlator with provision for variation between 3 and 6. The values of K' given in Table 7.1 are easily achievable in tilted plane processors. With these values we would obtain a unity output aspect ratio *and* would include a slant-range-to-ground-range conversion.

8. RECORDING POSITIONAL ERROR AND VELOCITY STABILITY

Both the range and the azimuth signals are linear FM signals and therefore will have similar restrictions on the positional error and velocity stability of the recording. However, the form of the recording is quite different for each. In range, the recording is periodically repeated over a relatively short distance. It is possible to measure and record the positional error along the scan. Thus, positional error is a useful measure for the range dimension although velocity measurement is equally valid. In azimuth, the recording is made continuously along the length of the film. Measurement of positional error is somewhat difficult to measure. It is relatively simple, however, to measure velocity error.

8.1 RANGE - CRT SWEEP

The range signal is recorded by means of an electron beam sweeping across the phosphor of the CRT. The deflection r_c in the range dimension is related to sweep time t' by

$$r_c = v_{co}t' + \varepsilon_c(t') \tag{8.1}$$

where v_{co} is a constant velocity and $\varepsilon_c(t')$ is a time varying positional error as illustrated in Figure 8.1.

For this discussion of sweep errors, the centre of the CRT screen of width W is defined as $r_c = 0$. The instant at which the beam crosses the centre is chosen at $t' = 0$. By selecting this reference, the deflection error is

$$\varepsilon_c(0) = 0 \tag{8.2}$$

at the centre of the CRT as shown in Figure 8.1(a).

The beam velocity is

$$v_c = v_{co} + e_c(t') \tag{8.3}$$

where v_{co} is a constant velocity and $e_c(t)$ is the velocity error as illustrated in Figure 8.1(b). The velocity is found from the deflection by

$$v_c = dr_c/dt' = v_{co} + d\varepsilon_c(t')/dt'. \tag{8.4}$$

Any small constant error in velocity can be corrected for by appropriate refocussing of the correlator during image processing. Therefore the slope of the best fit straight line on the deflection curve is taken as the ideal constant velocity v_{co}. Only the time-varying velocity error $e_c(t)$ will be considered as contributing to image degradation. Also note that the deflection error $\varepsilon_c(t')$ may usually be expanded into a polynomial such that $d\varepsilon_c(t')/dt' = 0$ at $t' = 0$. Therefore, the velocity error will be taken as

$$e_c(0) = 0 \tag{8.5}$$

at the centre of the CRT (see Figure 8.1(b)).

Several methods have been proposed for measuring both $e_c(t')$ or $\varepsilon_c(t')$. Below, the degradation of image quality caused by these errors will be discussed and limits on their value thereby determined. One measure of positional error used by some manufacturers is the "linearity error" defined by

$$L_c = \frac{\varepsilon_{cmax}}{W} \tag{8.6}$$

where ε_{cmax} is the maximum positional error over the entire sweep width W.

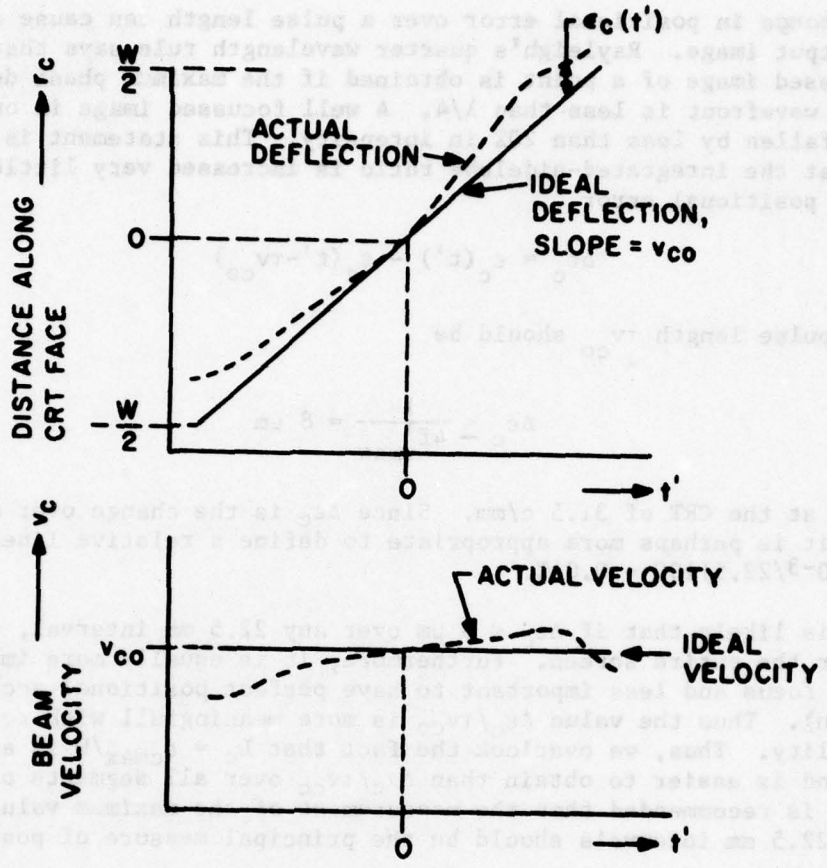

Figure 8.1. Ideal and Actual Deflection Characteristics Versus Time for a) Deflection and b) Velocity

The range signal is a linear FM pulse of duration τ = 33.8 μs and bandwidth B_r = 19 MHz. Range offset is employed such that the maximum frequency f_{max} = 21 MHz is only slightly greater than B_r. On film, the maximum spatial frequency is $f_{rmax} = f_{max}/v_c$, and the pulse width is τv_c. At the CRT the beam velocity is $v_{co} = 1.36 \times v_c = 6.66 \times 10^5$ mm/s and the pulse length is τv_{co} = 22.5 mm (0.89 inches). The 1.36 is the magnification of the relay lens. The maximum spatial frequency is $f_{rmax} = f_{max}/v_{co}$ = 31.5 c/mm.

A group positional error, i.e., a shift of one pulse as a block, results in a positional shift of the output image (distortion) but still gives a focussed image. The average positional error ε_{cav} over any pulse length τv_{co} causes a positional error of the image by the amount ε_{cav}. This shift of the image in range may or may not be considered serious by the user. If, for example, it is required to have a positional accuracy of the range image of 1/2 a resolution cell, then it is required that the maximum positional error for any 22.5 mm section be limited by $\varepsilon_{cmax} < 1.36 \times (25 \times 10^6/M_{rc})/2q \approx 21$ μm for a slant-range resolution of $25/M_{rc}$ m where M_{rc} is given in Table 5.1. The linearity error must be

$$L_c < \frac{21 \times 10^{-3} \times 100}{108} = 0.02\%. \qquad (8.7)$$

A *change* in positional error over a pulse length can cause a defocussing of the output image. Rayleigh's quarter wavelength rule says that a reasonably well focussed image of a point is obtained if the maximum phase deviation from the ideal wavefront is less than $\lambda/4$. A well focussed image is one where the peak has fallen by less than 20% in intensity. This statement is similar to saying that the integrated-sidelobe ratio is increased very little. Thus, the *change* in positional error

$$\Delta\varepsilon_c = \varepsilon_c(t') - \varepsilon_c(t'-\tau v_{co}) \tag{8.8}$$

over one pulse length τv_{co} should be

$$\Delta\varepsilon_c \leq \frac{1}{4f'_{rmax}} \approx 8\ \mu m \tag{8.9}$$

for f'_{rmax} at the CRT of 31.5 c/mm. Since $\Delta\varepsilon_c$ is the change over any 22.5 μm interval it is perhaps more appropriate to define a relative linearity measure of $(8 \times 10^{-3}/22.5)100 = 0.04\%$.

It is likely that if $\Delta\varepsilon_c < 8$ μm over any 22.5 mm interval, then $\varepsilon_{cmax} < 21$ μm over the entire screen. Furthermore, it is usually more important to have good focus and less important to have perfect positional accuracy (no distortion). Thus the value $\Delta\varepsilon_c/\tau v_{co}$ is more meaningfull with respect to image quality. Thus, we overlook the fact that $L_c = \varepsilon_{cmax}/W$ is a standard measure and is easier to obtain than $\Delta\varepsilon_c/\tau v_{co}$ over all segments of length τv_{co}. It is recommended that the measurement of the maximum value of $\Delta\varepsilon_c$ over all 22.5 mm intervals should be the principal measure of positional linearity.

An equivalent measure of $\Delta\varepsilon_c/\tau v_{co}$ can be made by measurement of velocity error. If the average velocity error e_{cav} can be obtained over each aperture length τv_{co}, then $\Delta\varepsilon_c$ is found from

$$e_{cav} = d\varepsilon_c/dt \simeq \frac{\Delta\varepsilon_c}{\tau} \tag{8.10}$$

from which the restriction

$$e_{cav} \leq \frac{v_{co}}{4f_{max}\tau} = 0.014\ \text{mm/s}$$

is obtained. The velocity stability criterion may be expressed as

$$\frac{e_{cav}}{v_{co}} \simeq \frac{\Delta\varepsilon_c}{\tau v_{co}} \leq \frac{1}{4f_{max}\tau} = 0.04\% \tag{8.11}$$

where $f_{max}\tau$ is approximately the time-bandwidth product. Thus, over any 22.5 mm section of CRT, the average velocity error should not exceed 0.04% of the mean velocity v_{co}.

For high resolution operation, magnetic deflection is used almost exclusively. As pointed out in [2], the main deflection non-linearity in magnetically deflected CRT's, arises from the relation [3]

$$I = K \sin \gamma \tag{8.12}$$

where γ is the electron beam's deflection angle, K is a constant and I is the current through the deflection coil. Note that

$$\sin \gamma = \frac{r_c}{\sqrt{R_1^2 + r_c^2}} \tag{8.13}$$

where R_1 is the distance between the electron gun and the screen. Upon expansion

$$I = \frac{K}{R_1}\left[r_c - \frac{r_c^3}{2R_1^2} + \frac{3r_c^5}{8R_1^4} \cdots\right]. \tag{8.14}$$

The first term is the desired linear deflection relation and the remaining terms are the nonlinear deflection error. As an example, consider $R_1 = 12$ inches and for our work $r_{cmax} = 4.25/2 = 2.1$ inches. Note that the error is greater the further the spot is from $r_c = 0$. Consider only the cubic and fifth order error terms. The pulse width of 33.8 μs is 22.5 mm (0.89 inches) on the CRT screen. Therefore, the change is positional error L_{c2} over this width at the worst location is

$$\Delta\varepsilon_c = \frac{2.1^3 - 1.21^3}{2 \times 12^2} + \frac{3(2.1^5 - 1.21^5)}{8 \times 12^4}$$

$$= 2.6 \times 10^{-2} + 6.9 \times 10^{-4} = 2.7 \times 10^{-2} \text{ inches}$$
$$(678\ \mu m)$$

The fifth power term is negligible compared to the cubic. The cubic is seen to be much larger than the minimum permissible change in positional error $\Delta\varepsilon_c < 8.0$ μm.

Such a nonlinearity can conceivably be corrected by appropriately modifying the current ramp used to drive the deflection coil. In fact, ERIM has done this [2] by dividing the scan across the CRT into eight segments and providing a separate adjustment for each segment. The above nonlinearities are not the only ones arising in the deflection. Coil imperfections, resonances, etc., will give rise to deviations from a perfect scan. These imperfections cannot easily be predicted and must be measured after construction of the CRT system.

A promising approach to sweep correction was used by Bousky and Teeple [4] for correcting a laser scanner recording on moving film. They used a simple preprogrammed ROM to provide spatial error compensation in two orthogonal directions for a 16 MHz bandwidth signal. This compensation permitted them to use a somewhat lower quality multi-faced rotating mirror and therefore a much lower cost. They achieved error offsets in *both*

dimensions of less than 1% of *the spot size*. Clearly, the same preprogramming of a ROM for spatial error compensation is perhaps even easier to apply to CRT scanning. In fact JPL are using a PROM to provide 256 corrections of the slope of their CRT sweep. Note that this method is particularly useful in cancelling the residual nonlinearities mentioned previously arising from peculiarities of the particular yoke, CRT, etc..

Determination of the sweep error may be found a number of ways. At ERIM [2], a reference precision grating was superimposed on the CRT and a test pattern generated on the screen. Sweep defects would then be visible to the eye. An extension of this technique [5] involves imaging the CRT scan on to a precision Ronchi ruling. If the relay lens to be used in the actual recording is used, then positional errors due to the lens will also be measured. Behind the Ronchi ruling is a photodetector connected to a counter whose output is proportional to position. Alternatively, the CRT could be imaged on to a precision multi-element photodetector such as are found on optical multichannel analyzers (one such instrument is already available at CRC).

8.2 AZIMUTH - FILM VELOCITY

The azimuth signal is recorded by film moving past the image of the CRT at a velocity

$$v_f = v_{fo} + e_f(t) \tag{8.15}$$

where $e_f(t)$ is the time varying velocity error and v_{fo} is the average velocity which has components

$$v_{fo} = v_{fd} + e_{fo} \tag{8.16}$$

where v_{fd} is the desired constant velocity and e_{fo} is a constant error velocity. Upon processing, the constant velocity error e_{fo} results in a scale change and in a defocussing of the output azimuth image. However, the scaling and defocussing may be corrected for by adjustment of the optical correlator. Therefore a constant velocity error may be tolerated provided a very accurate measure of v_{fo} is made to aid in the focussing of the correlator. Hereafter, only the time varying velocity error $e_f(t)$ will be considered as contributing to image degradation.

The position along the film is

$$\begin{aligned} x_f &= v_{fo}t + \int e_f(t)dt \\ &= x_{fo} + \varepsilon_f(t) \end{aligned} \tag{8.17}$$

where x_{fo} is the expected position and $\varepsilon_f(t)$ is the time-varying positional error. Again, a constant error in x_{fo} results in only a constant offset of the azimuth image. It will not be considered here as an image degradation.

Usually, magnetic tape drive stability is measured in terms of "flutter" $\Delta v_f(f)/v_{fo}$ where $\Delta v_f(f)$ is the rms velocity error in a 1 Hz bandwidth. However, it does not appear convenient to measure the film drive stability in this manner. Two more-appropriate methods are now suggested. The first method is an indirect one. A shaft-angle encoder will be part of the film-drive servo. The difference signal between its output and a reference oscillator gives an indication of the capstan rotational position error and hence gives some indication of the film's positional error $\varepsilon_f(t)$. Differentiation,

$$d\varepsilon_f(t)/dt = e_f(t) \tag{8.18}$$

gives the velocity error $e_f(t)$. In the second method a stable sine wave is generated and recorded along the azimuth direction. The recorded film is optically Fourier transformed. A small velocity error over a relatively short section will appear as a small shift of the transform. With the knowledge that only these two measures of stability are available, stability requirements are derived below.

A group positional error, i.e., the constant shift of one entire synthetic aperture recording, results in a positional shift of the output image (distortion) but still gives a sharp image. Usually the user can tolerate such a shift within reason and is therefore neglected. However, a positional error that changes during a synthetic-aperture length can cause a defocussing and with multiple look processing can cause the various looks to be offset from each other giving rise to blurring. The $\lambda/4$ rule says that the highest spatial frequency f_{xmax} should have a positional error of less than 1/4 of its wavelength over the aperture. The aperture length in time, T_a or on film, $T_a\, v_{fo}$ is the full synthetic aperture for 1 look operation and is the total aperture of all looks for multiple look operation. The apertures for 3 cases are given in Table 8.1. Thus, $\Delta\varepsilon_f$, the *change* in positional error over a aperture length $T_a\, v_{fo}$, should be limited to

$$\Delta\varepsilon_f < \frac{1}{4f_{amax}} \tag{8.19}$$

where $f_{xmax} = f_{dmax}/v_{fo}$ and f_{dmax} is the maximum doppler frequency. The maximum doppler frequency is taken to be 1/2 the doppler bandwidth. The frequency offsets due to pitch, yaw and "equivalent yaw" are neglected because in the subsequent optical processing a beam steering technique is used that cancels most of the image degrading effects of this frequency offset. The resulting values of $\Delta\varepsilon_f$ are given in Table 8.1.

A change in positional error implies a velocity error. If the average velocity error e_{fav} can be measured over the aperture length $T_a v_{fo}$, then $\Delta\varepsilon_f$ may be computed from

$$\Delta\varepsilon_f \simeq T_a e_{fav} \tag{8.20}$$

from which the restriction

TABLE 8.1

Positional and Velocity Error Limits for Film Drive

Mode of Operation		Aperture Time T_a	Aperture Length on Film $T_a v_{fo}$	Highest Doppler Frequency f_{max}	Change in Positional Error $\Delta\epsilon_f$ should be Less Than	Velocity Error e_{fav} should be Less Than	$\frac{\Delta v_f}{v_{fo}} \times 100$
Resolution	Looks						
6.5 m	1	2.0s	80.0 mm	1040/2 Hz	19.2 μm	9.6 μm/s	0.02%
25 m	4	2.0s	80.0 mm	1040/2 Hz	19.2 μm	9.6 μm/s	0.02%
25 m	1	0.52 s	20.8 mm	273/2 Hz	73.3 μm	140 μm/s	0.35%

$$e_{fav} < \frac{f_{vo}}{4f_{dmax}T_a} \tag{8.21}$$

is obtained and is listed in Table 8.1. It is not appropriate to express positional stability in terms of a percentage. The restriction on the velocity stability, however, can usefully be expressed as

$$\frac{\epsilon_{fav}}{v_{fo}} \leq \frac{1}{4f_{dmax}T_a} \tag{8.22}$$

where $f_{dmax}T_a$ is 1/2 of the time-bandwidth product. The velocity stability ratio is given in Table 8.1.

From Table 8.1 it is seen that for 6.5 m resolution or for 4-look operation both the maximum positional error and the velocity stability are very restrictive. For 25 m resolution, 1 look, the restrictions are greatly relaxed.

It may be useful to use a feedback system to add a slight deflection in the *azimuth* direction to the electron beam. This form of spatial error compensation was used on the analogous laser beam recorder described in [4].

Our film drive requirements have three factors that simplify design and construction. First it has a nearly fixed speed whereas other film drives have large velocity variation capability. Second, the film is moving relatively fast - 40 mm/s. Therefore, extensive gearing down, required by low velocity drives, is not required. The third factor is that the drive will be ground based on a vibration-isolated table and in a clean atmosphere. Many previous film drives were required to operate airborne.

8.3 FILM VELOCITY VARIATION WITH LATITUDE

The lower and upper latitudes between which the Shoe Cove station can receive reasonably good signals (assuming a 10° antenna angle) are $\phi_{lat} = 29°$ and $\phi_{lat} = 66°$. In transversing this distance, both the altitude h_s and the satellite velocity, V, changes. The azimuth signal has a scale factor

$$p = \frac{V/c_a}{v_f} \quad . \tag{8.23}$$

Since both V and $c_a = 1-h_s/re$ vary with latitude, the scale factor p will vary if v_f is held constant. In a companion report [6] the maximum phase error in the azimuth dimension resulting from holding v_f constant over the viewing area of Shoe Cove was determined and is summarized here in Table 8.2. From Rayleigh's $\lambda/4$ rule the number of times the correlator would have to be refocussed over one pass is about 3 for 4 look operation and would not require any refocussing for 1 look, 25 m-resolution.

Instead of refocussing the correlator as a pass progresses, one could vary v_f during the pass so as to keep p constant. It could be varied continuously as appears to be the case for the JPL recorder or it could be corrected in discrete steps - a maximum of 3 changes being required. If the film velocity v_f is exactly 40.0 mm/s at the centre of one pass then the film velocity should vary as shown in Table 8.3. A maximum swing of ±0.1% in velocity is required - probably not particularly difficult to obtain in practice.

TABLE 8.2

Maximum Phase Error Over One Pass Arising from Latitude Dependent Changes in V/c_a

Azimuth Resolution	Number of Looks	$\phi_e\|_{max}$	$\phi_e\|_{max}/(\pi/2)$
6.5 m	1	5.0 radians	3.2
25 m	4	5.0	3.2
25 m	1	0.3	0.2

TABLE 8.3

Value of v_f as Latitude Changes for Constant p

Latitude	V/c_a	v_f for p Constant
29°	6796 m/s	40.04 mm/s
66°	6783 m/s	39.96 mm/s
% change	0.2%	0.2%

9. EXPOSURE

In this chapter the amount of light available at the film is calculated. In radiometric units, the exposure E of photographic film is just the energy density, in ergs/cm^2 or joules/m^2, which falls on the film. Photometric units are not of use here. The exposure is given by

$$E = Ht \tag{9.1}$$

where H is the power density (irradiance in watts/cm^2 or watts/m^2) and t is the exposure time. Therefore to calculate the exposure it is necessary to calculate the transfer of power density between CRT screen and film rather than the total power transfer.

In Figure 9.1, an elemental area of power density H_o is imaged on to an elemental area of film. From considerations such as found on p 188ff of [7] the power density H_1 at the film may be shown to be

$$H_1 = \eta H_o \sin^2\theta_1 = \eta H_o(\sin^2\theta_o)/M^2 \qquad (9.2)$$

where η is the intensity transmittance of the imaging system, and θ_o and θ_1 are, respectively, the entrance and exit pupil half-field angles. The magnification is

$$M = \frac{\sin\theta_o}{\sin\theta_1} . \qquad (9.3)$$

For a relay lens of focal length F,

$$H_1 = \frac{\eta H_o}{4(f/no)^2(1+M)^2} \qquad (9.4)$$

where the so-called f-number is

$$f/no = F/a \qquad (9.5)$$

and a is the diameter of the entrance when the object is at *infinity*. In our application the object is not near infinity and in such cases an effective f-number is sometimes used and is defined by

$$f/no|_{eff} = (f/no)(1+M) = \frac{1}{2\sin\theta_1} . \qquad (9.6)$$

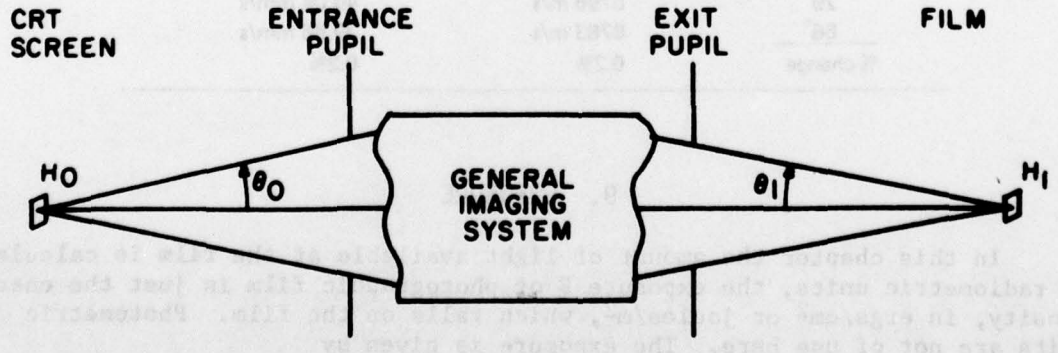

Figure 9.1. General Imaging System for Power-Density Transfer Calculations

The power density H_o scattered forward from the phosphor is

$$H_o = \frac{I_b V_b \eta_{crt}}{Ld} \tag{9.7}$$

where I_b is the beam current and V_b is the beam voltage. The area of the trace is Ld where L is the trace length and d is the spot size. The CRT efficiency η_{crt} is the ratio of total light power emitted from the face plate into air to the incident beam power $I_b V_b$. Because η_{crt} is determined by measuring total emitted light power, it includes all possible factor affecting light output including aluminizing of the phosphor. All CRT's under consideration for our application are aluminized so as to reflect all emitted light into the forward direction.

The exposure time for the entire trace at the film is ML/v_{co}. Thus, the exposure at the film is

$$E_1 = \frac{I_b V_b \eta_{crt}\, \eta}{4(f/no)^2(1+M)^2} \frac{M}{dv_{co}} . \tag{9.8}$$

The exposure levels produced by two CRT candidates are now estimated. The candidates are modified CRT's from the CRC/DND APS-94D radar and two Infodex PD1200 CRT systems. The relevant characteristics are given in Table 9.1. Efficiencies η_{crt} of 2 to 3% are typical for P11 phosphors. Here 1% is used in the calculation. The magnification is M = 1/1.36 = 0.74 and v_{co} = 4.90 x 10^5 mm/s. A typical lens transmission of η = 0.8 is used. An f/2.0 lens is under design and construction. Temporarily, a lens of perhaps f/4.0 capability may be used. The estimated energy density E_1 available to expose the film is given in Table 9.1 for these two f numbers. Units are in ergs/cm^2 where 10^7 ergs = 1 joule (watt-sec).

TABLE 9.1

Estimates of Available Energy Density (Exposure) at Film Plane

Characteristic	Modified APS-94D	Infodex PD1200
phosphor type	P11	P11
I_b	assumed 1 μa	1 μa
V_b	12 kV	25 kV
d	0.7 mil = 17.8 μm	0.7 mil = 17.8 μm
E_1 for f/4.0 lens	0.042 ergs/cm^2	0.087 ergs/cm^2
E_1 for f/2.0 lens	0.17 ergs/cm^2	0.35 ergs/cm^2

10. RECORDING FILM SELECTION

There has been considerable collaborative work with B. Young and J. Salt of DREO on the selection of a photographic film for the recorder. At this writing it has been decided to order 4 of the more likely film candidates, try them all in the recorder, and compare their results. In the following sections various characteristics of these films are compared. The comparison is summarized in Table 10.2 at the end. Many other films had, of course, been studied but rejected for various reasons.

The films ordered for further study were all Kodak films; types RAR2494, RAR2498, Tri-X Pan (5063), and SO-201. The SO-201 (SO = "special order") is apparently the same as RAR3494. RAR stands for "rapid-access recording".

10.1 RESOLUTION

It was seen in Section 6 that the maximum range spatial frequency that must be recorded by the film is 42.9 ℓp/mm. In azimuth, the resolution was expressed in terms of spot size. The film should be able to record a 12 μm spot. A 12 μm gaussian spot has a spectrum that falls to 50% at 36.7 ℓp/mm. Thus it is desired to find a film with good MTF out to at least 43 ℓp/mm.

MTF curves were obtained from Kodak for all the films under consideration. Rather than reproduce them here, the MTF at certain selected spatial frequencies are given in Table 10.2. The flatness of the MTF is also important. An indication of flatness is given by the change ΔMTF in MTF between 10 and 40 ℓp/mm. RAR3493 appears to be one of the flatest with a variation from 77% to 54% (1.5 dB) but also has an unexplained overall constant loss in MTF of about 23% (-1.1 dB). The worst fall of amongst the 4 under consideration is the Tri-X with a maximum of 103% and minimum of 60%, a variation of 2.3 dB.

10.2 SENSITIVITY - t_a-E CURVES

The data film (interferogram) is one element of a linear system. If linearity is to be maintained through the optical system, then it is essential that the linear portion of the amplitude transmittance versus exposure curve (t_a-E curve) be utilized. If modulation extends into the nonlinear region, the intermodulation may fall within the correlator's passband.

Usually the t_a-E curve for films are not available from the manufacturer whereas the density versus log-exposure (D-log E) curves are. Conversion from a D-log E curve to a t_a-E curve is calculated from

$$E = 10^{\log E} \tag{10.1}$$

and

$$t_a = (10^{-D})^{\frac{1}{2}} = 10^{-D/2}. \tag{10.2}$$

The square root in (10.2) comes from the fact that t_a is amplitude transmittance whereas $D = \log(1/\tau)$ where τ is the intensity transmittance. The

results are shown in Figures 10.1 and 10.2. For the exposures given in ergs/cm^2 the exposures were made with light whose spectrum simulated that of a P11 phosphor. Unfortunately the exposures for some films were only given in meter-candles second and used either tungsten light or daylight. This measure cannot be directly compared to the desired radiometric measure in ergs/cm^2. Thus, the curves in Figure 10.2 are only useful for a comparison of the films used in this figure but has little use in the determination of P11 phosphor exposure requirements.

The interferogram is recorded as the desired signal plus a bias. The bias is chosen to be close to the middle of the most linear section of the fast rising section of the t_a-E curve. The bias value of t_a is typically between 0.4 and 0.7. Note that such values of t_a correspond to the toe of the D-log E curve. Fortunately, this means that the film will be operated at the low exposure end of its operating range. The bias average density will therefore be low so that the interferogram will have a rather "washed-out" light-gray appearance. As a basis for comparison, a value of $t_a = 0.5$ was selected as a typical bias level. The corresponding density is $D = 0.6$. The exposures required to obtain $D = 0.6$ are given in Table 10.2 along with exposures to obtain $D = 0.1$ and $D = 1.0$. Unfortunately some of the exposures were available only in photometric units of mcs. A few were given in both in such a manner that by using a linear interpolation an approximate radiometric value was obtained.

10.3 FILM SIZE

The signal width on the film is 4.25/1.36 = 3.13 inches (79.4 mm) and room is required for annotation and edge guiding. Five inch film was decided upon. The Kodak S-33 spool will be used. In Section 7.2 it was seen that a maximum of 79 ft. (24m) of film is needed for a 10 min. pass.

10.4 REVERSAL FILMS

Certain films such as RAR2498 are capable of reversal processing to produce a positive transparency. It appears that the MTF is not degraded by reversal processing. The advantage of a reversal film arises in the azimuth direction wherein, under ideal conditions, there are gaps between the sample points. For negative films these gaps are transparent and therefore admit extra background light into the correlator. This background contributes significantly to the noise of the correlator. For a positive transparency, the gaps are opaque and therefore block unwanted light.

Figure 10.3 shows the t_a-E curve for RAR2498 film with reversal processing. The bias point would be at about $t_a = 0.5$ as with negative form. Unfortunately the exposure is given in photometric rather than radiometric units. It is therefore difficult to compare exposures between the negative and reversal films. It would appear that ergs/cm^2 and mcs are moderately close in value so that perhaps exposure given in Figure 10.3 may be compared approximately to that given in Figure 10.2. In that case, the exposures required in both cases are about the same.

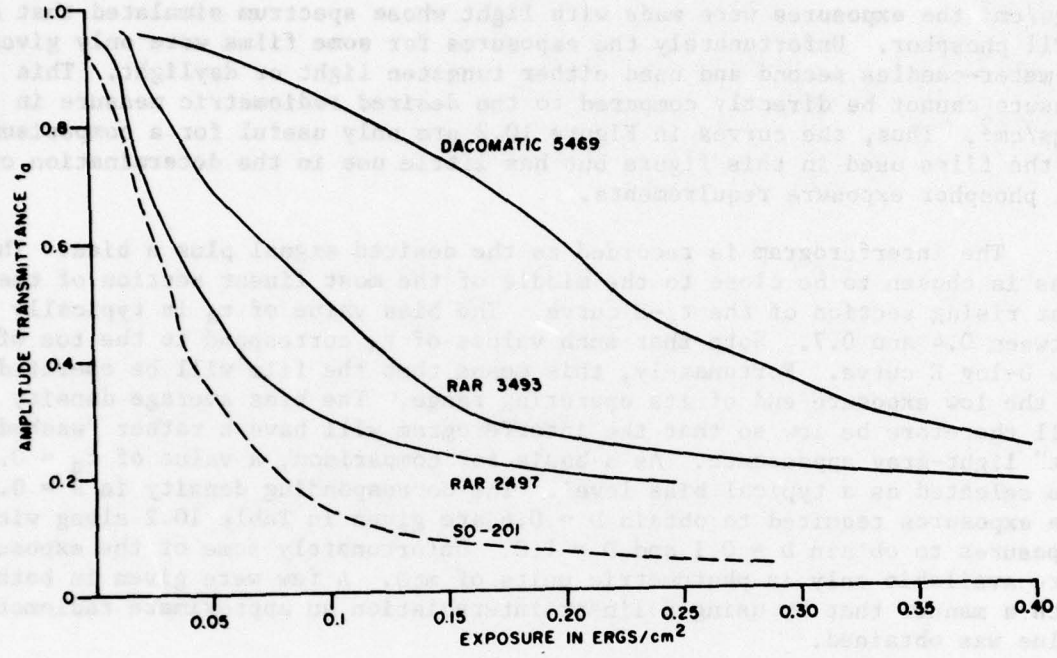

Figure 10.1. t_a-E Curves for RAR2497, RAR3493, Dacomatic 5469, and SO-201

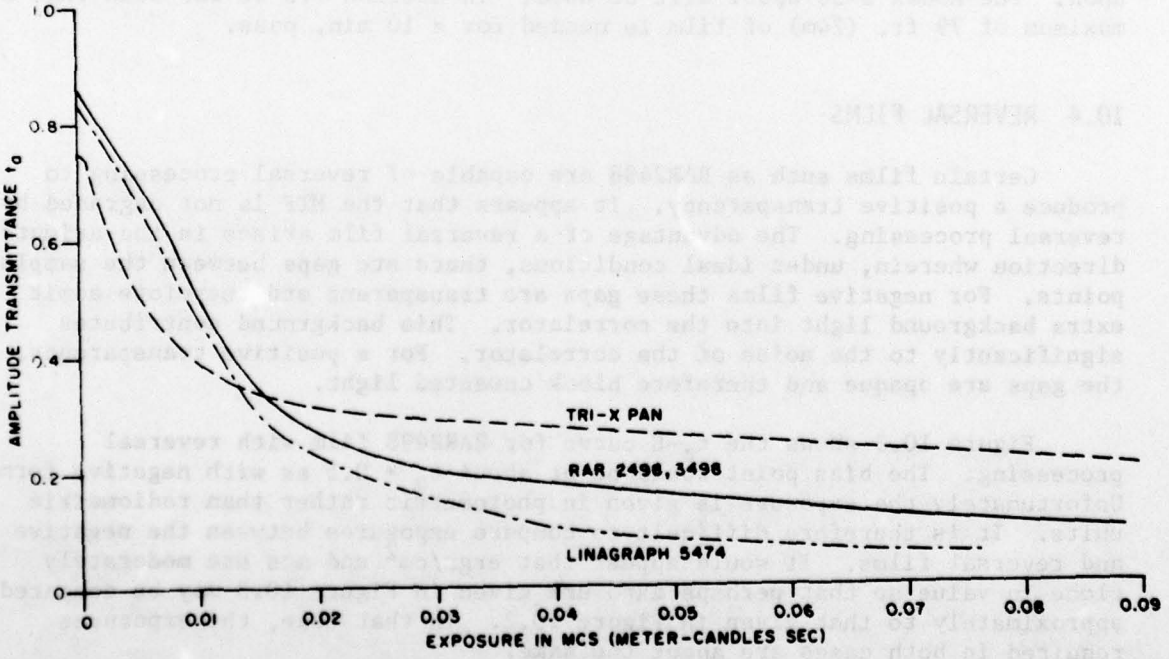

Figure 10.2. t_a-E Curves for RAR2498, and Tri-X Pan and 5474

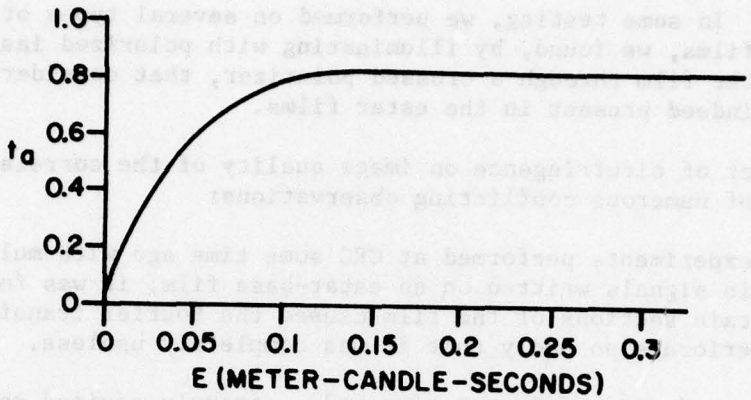

Figure 10.3. t_a-E Curve for RAR2498 Film Under Reversal Processing

It is to be noted that the bias, $t_a = 0.5$, corresponds to a point that is close to the toe region of the D-log E curve. However, for a reversed film the toe is in the region of *highest* exposure. This unfortunate fact may be offset by the fact that a reversed film may have higher overall sensitivity. Note that reversal processing involves more steps than does normal (negative) processing.

10.5 FILM BASE AND BIREFRINGENCE

The two common bases of photographic film used today are acetate and polyester films. The polyester film used is a form of Mylar for which Kodak uses the trade name "Estar". Apparently Kodak uses a four number coding system for its films wherein the first number indicates film base type and thickness. The three combinations of interest are given in Table 10.1. It is assumed that the remaining 3 numbers describe the emulsion. Thus RAR2498, 3498 and 5498 have the same emulsions but differ in film base.

During the manufacture of estar, there is a stretching that leads to randomly oriented internal stresses. These stresses cause the film to be birefringent (doubly refracting). The effect is related to stress induced photoelasticity. The stress is randomly distributed, and therefore so is the birefringence. When estar-based films are used in polarized light, such as obtained from most lasers likely to be used for the correlator, a spatially random modulation of the polarization is introduced by the bire-

TABLE 10.1

Number Coding for Kodak Films

First Number	Film Base	Film Thickness	Examples
2	estar	4.0 mils	RAR2498
3	estar thin	2.5 mils	RAR3493
5	acetate	5-1/4 mils	Tri-X 5063, Shell burst 5474

fringence [8]. In some testing, we performed on several types of estar and acetate-based films, we found, by illuminating with polarized laser light and observing the film through a crossed polarizer, that considerable birefringence was indeed present in the estar films.

The effect of birefringence on image quality of the correlator is not clear because of numerous conflicting observations:

(a) In experiments performed at CRC some time ago with multichannel audio signals written on an estar-base film, it was found that certain sections of the film caused the Fourier transform to deteriorate so badly that it was completely useless.

(b) Thomas Herman of Data Optics Ltd., strongly advised against estar-based films. He has had many years experience at ERIM and ERIM always avoids estar films.

(c) Goodyear, in their AN/UPD-4, uses an estar-based film for recording interferograms and with good success.

(d) Little effect was noted in [8] in using estar film for the matched filter in a Vander Lugt filter form of correlator.

In DREO memo 3390-2-7 of 23 February 1978, J. Salt describes results of experiments that go a long way to predicting the effect of the use of estar films. The present DREO correlator was set up with a high quality interferogram (on acetate base) in the input and the resulting image recorded. Clear pieces of 2.5 mil estar, 4.0 mil estar and acetate film were then, in turn, superimposed on the interferogram and the resulting image recorded and compared. Without index matching fluid in the liquid gate, the estar films considerably reduced the contrast of the output image. With index matching fluid the image quality for all cases was not much different than the original reference image. The acetate-base film, caused a small decrease in contrast perhaps because of the presence of the blue antihalation dye in the base. Neither rotation nor stretching of the clear estar films seemed to make much difference to the image quality. These experiments implied that with proper index matching, estar base films were suitable for the interferogram.

Finally note that with estar-based films, the appearance of unexposed and developed film varies from very transparent and clear to moderately gray. It would seem that the clear types may be more useful. In general the acetate films have a higher base fog, which could be a drawback.

10.6 DISCUSSION

The comparisons in Table 10.2 must be very carefully interpretted. The information can be very misleading and inaccurate. For example, MTF and sensitivity were not necessarily determined under the same conditions. It is likely that sensitivity and MTF were measured under best conditions for each and as a result the MTF's and the sensitivities quoted cannot usually be achieved simultaneously. Secondly, some of the sensitivity measurements were in photometric units which are difficult to compare to the desired radiometric units based on P11 phosphor illumination.

TABLE 10.2

Some Characteristics of Films Being Considered for the Recorder

Film Type	Comments	Exposure[1] Required to Give a Density of: D = 0.1	D = 0.6	D = 1.0	ASA Rating	MTF in % Spatial Freq. ℓp/mm 10	20	30	40	ΔMTF in % Between 10 ℓp/mm and 40 ℓp/mm	Diffuse Rms Granularity[4]	Film Base
RAR 3493	Used by Goodyear for most of their interferogram recording and by JPL for recording SEASAT.	0.22 $\frac{ergs}{cm^2}$	0.10 $\frac{ergs}{cm^2}$	0.16 $\frac{ergs}{cm^2}$	50	77	70	62	54[2]	23	20	Estar-thin (2.5 mils)
RAR 2498	Can be reverse processed. Is used by Goodyear for recording correlator output.	0.016 $\frac{ergs}{cm^2}$	0.008 mcs ≃0.035 $\frac{ergs}{cm^2}$[5]	0.018 mcs 0.083 $\frac{ergs}{cm^2}$	250	97	90	78	64	33	28	Estar (4.0 mils)
DACOMATIC G 5469	Suggested by R. Anwyl of Kodak	0.07 $\frac{ergs}{cm^2}$	0.22 $\frac{ergs}{cm^2}$	0.33 $\frac{ergs}{cm^2}$		91	89	78	68	23	9	Acetate (5-1/4 mils)
TRI-X-PAN 5063	With Gray Antihalation Base — Clear Base —	Below Fog Below Fog	0.005 mcs 0.014 mcs	0.025 mcs 0.040 mcs	400	103	90	73	60[3]	43	28	Acetate (5-1/4 mils)
LINAGRAPH SHELLBURST 5474	Suggested by Pisconski of Kodak.	Below Fog Below Fog	0.009 mcs ≃0.058 $\frac{ergs}{cm^2}$	0.015 mcs 0.1 $\frac{ergs}{cm^2}$		100	86	70	53	47	24	Acetate (5-1/4 mils)
SO-201 (3494)	Used by The APS-94D recorder. Estar-thin base (2.5 mils)	0.004 $\frac{ergs}{cm^2}$	0.035 $\frac{ergs}{cm^2}$	0.060 $\frac{ergs}{cm^2}$		86	81	71	62	24	24	Estar-thin (2.5 mils)

1. Exposures given in ergs/cm^2 are for exposures made with simulated P11 phosphor light. Exposures given in meter-candles second (mcs) are for either tungsten light or daylight. Thus the two measures cannot be directly compared.

2. The MTF curve for RAR 3493 had a peak of only 77% (occurring at 10 ℓp/mm). It is sufficiently anomalous that it is not clear if this is a true representation or a mistake in plotting by Kodak.

3. The MTF for Tri-X goes to approximately 110% at 5 ℓp/mm so that the fall off in MTF is slightly greater than implied by number in above table.

4. This value is 1000 times the standard deviation of the density scanned with microdensitometer with a 49 μm diameter aperture.

5. For RAR 2498 and Linagraph 5474, exposure indices in the reciprocal of ergs/cm^2 were given for densities of 0.1, 1.0 and 2.0. However, the characteristics curves are given in mcs and are for the tungsten or daylight illumination. A linear relation between ergs/cm^2 and mcs are assumed, the proportionality constant determined for densities D = 1.0 and 2.0, and the exposure for ergs/cm^2 at D = 0.6 thereby calculated.

One usually assumes that there is always a trade off between resolution and sensitivity. In our study the following unusual observation has been made. It was found that, except for very slow films, the MTF curve of various films varies relatively little over a fair range of film sensitivities. Similarly film granularity did not seem to be closely related to MTF. However the subjective image quality of films used in normal cameras does seem to be related to granularity. Kodak representatives could not explain these phenomena. This subject deserves further study. As a result of this observation the tendency was to go for the more sensitive films since little was lost in MTF.

An idea of the sensitivity requirements is obtained by, first, using, Table 10.2 to find the exposure required to give a density of 0.6 (t_a=0.5). Then the estimated available exposure light is obtained from Table 9.1 for 4 combinations of f-number and CRT. The numbers given in both tables are not particularly reliable so it would be preferable to have a good safety margin in exposure. It appears that both the RAR 3493 and Dacomatic G 5469 would be adequately exposed only with an f/2.0 lens. The 4 films chosen for further work all appear to be suitable for even the least exposure case of Table 9.1.

The RAR 3493 was abandoned not only because it was slow but because its absolute value of MTF was low (even though it was relatively flat). The Dacomatic G is too slow and the Shellburst 5474 was disappointing in general. Our first choice was the acetate base film RAR 5498 which, unfortunately, Kodak rejected as having pinholes in the 5" film we wanted. Because the problem of acetate versus estar is not fully resolved it was thought best to order samples of both estar and acetate based film. It was thought that 2.5 mil estar may show less birefringence than the 4.0 mil estar. SO-201 was selected as this representative. For comparison RAR 2498 film was chosen because it is the 4.0 mil estar version of the desired 5498. Kodak said they would look into the availability of the 2.5 mil version RAR 3498. RAR 2494 is the 4.0 mil version of SO-201 (3494). The acetate base film chosen was the Tri-X. It has a high MTF at lower frequencies but falls off the fastest of the 4 films.

11. LENS SELECTION

The recorder-lens must be able to image spatial frequencies of up to 42.9 ℓp/mm at the image plane (see Table 6.1) with little attenuation and to do this over a 80 mm width at the image. The lens should be f/4.0 or better. Such performance is very difficult to achieve.

The on-axis MTF of an aberration-free lens is a straight line between MTF=1 at 0 ℓp/mm to MTF=0 at the cut off frequency f_c where

$$f_c = \frac{a}{\lambda s'} = \frac{1}{\lambda (f/no)(1+M)} , \qquad (11.1)$$

M is the magnification, a the lens diameter (see Chapter 9), and s' is the lens to image distance. For example with λ = 632.8 nm and M = 1/1.36, f_c =

228 ℓp/mm for f/4.0 and f_c = 455 ℓp/mm for f/2.0. The MTF at 49.2 ℓp/mm is therefore 78% for f/4.0 and 89% for f/2.0. These values appear very good. Unfortunately, in practice the MTF falls (a) dramatically in the presence of even small aberrations and (b) as the image moves off axis. Often the MTF can be improved by *increasing* the f-number because the decrease in aberrations more than compensates for the decrease in f_c.

At this writing, two approaches are being taken. For the long term, the contractor is having designed and built a f/2.0 11-element lens of very high quality. It will likely have a field flattener placed near the image. As an interim lens, two camera lenses placed face to face are being considered. In this configuration both lenses are operating in a mode for which they were designed - one conjugate at or near the back focal plane and the other at infinity. Nearly parallel light will pass between the lenses. There are certain other advantages to operating in this mode. First, if individually the f-numbers are both F/no then the combined f-number is (F/no)/2 which is a significant gain. Secondly, two identical lens with a stop between them is free of distortion for unity magnification. A simple single element lens may be used to flatten the field if necessary. Initial measurements have shown that pairs of certain portrait lenses designed for 4" x 5" format or larger have good MTF over the 80 mm field we want.

The amount of curvature of field that can be tolerated depends upon the depth of focus. Depth of focus is difficult to predict. On page 486 of [7], are MTF curves for an aberration free lens with various amounts of misfocus. The depth of focus is then determined by placing some criterion on a minimum acceptable MTF curve. One criterion is to find the misfocus that causes the MTF at 43 ℓp/mm (at the image) to fall by 10%. Following this criterion a depth of focus of 25 μm (1 mil) is found for f/2.0 and 60 μm (2.4 mil) for f/4.0. The presence of aberrations will likely reduce the depth of focus.

12. MISCELLANEOUS

12.1 ANNOTATION

In addition to the main signal, certain other data must be recorded. The recording format for this additional data is discussed below. The discussion is preliminary and subject to revision since at the time when this document was written, the annotation and reference parameters had not been fixed.

The interferogram itself will be annotated as illustrated in Figure 12.1. For the purpose of range referencing, continuous lines, located about 1/2 inch from the signal region, will be drawn down both sides of the film.

Timing pulses, 1 ms wide and 100 ms apart, generate timing marks every 4.0 mm. Along the same line there is generated, every one minute, a time code that gives the time in seconds, minutes, hours, days and 100 days. The standard 36 bit NASA time code consists of 2 ms and 6 ms pulses, spaced 10 ms apart. The 2 [illegible] and 6 ms pulses indicate a "0" and "1" respectively. This

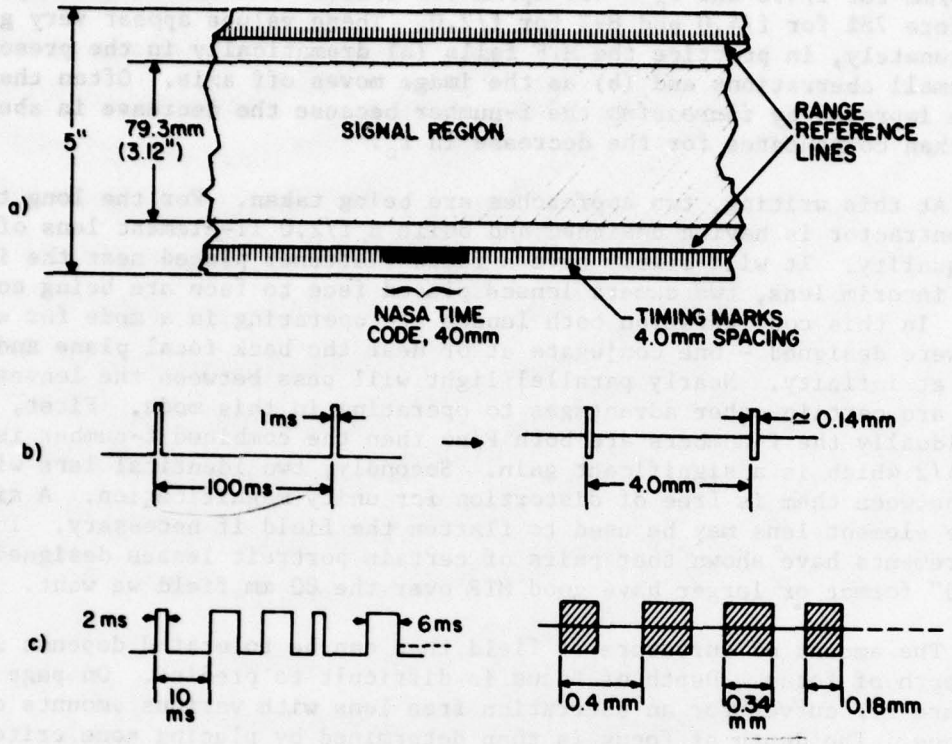

Figure 12.1. Annotation for Interferogram Film Showing a) The Interferogram b) The Timing Pulses and Resulting Timing Marks, and c) Time Code Pulses and Resulting Time Code Marks.

becomes the time code marks shown in Figure 12.1(c), where the spacing is 0.4 mm and the widths are 0.18 mm and 0.34 mm. It is intended to image a numeric character LED through a microscope objective onto the film. The decimal point will provide the continuous range reference line. One of the vertical bars will provide the timing marks and timing code marks. The recorded marks will not necessarily be as sharp as shown in Figures 12.1(b) and (c) so there may be difficulty in distinguishing between a short and a long mark. As regards LED size, microscope objective, etc., experimental work will have to be done to ensure that a readable time code is obtained.

Some of the data required by the correlator does not necessarily have to be recorded on the film. For example, the PRF is not expected to change during a pass so it would be sufficient to have its value handwritten on the film container. The time and amount of the range delay change could be annotated on the film. However, since only one or two changes per pass are expected, it would be sufficient to provide a printout giving the change as a function of GMT. The correlator operator would have to watch the time annotation to find the location of the change. If velocity feedback is not used during recording, a record of the satellite velocity vs GMT is necessary. Again this could take the form of a printout to be sent along with the unprocessed recording film. Note that the film velocity v_f is selected independent of PRF. Therefore it is *not* to be changed as PRF is changed.

12.2 TRIGGERING

It is extremely important to commence the sweep at exactly the same time after each transmission of a pulse. Precise trigger signals will be available from the SAR demodulator. The recorder must be made compatible with these trigger signals. Furthermore a precision delay must be available so that the second CRT can be triggered at the appropriate time relative to the triggering of the first CRT. The delay may be obtained either by a commercial device made for that purpose or by counting down the 45.5 MHz sample clock.

13. SUMMARY

Table 13.1 contains a summary of the specifications arrived at for the recorder and the film. The basic assumptions used when calculating the table were: 2 CRT's containing 2 subswaths each, a film velocity of 40 mm/s, and a beam velocity measured at the film of 4.90×10^5 mm/s. Everything in the table follows from these assumptions.

TABLE 13.1

Specifications for the Recorder and Film

Characteristic	Value	Relevant Section or Table
CRT		
nominal desired spot size	0.65 mil (16.5 μm)	
useful trace length	4.25 inches (108 mm)	
phosphor	P11	
beam current	$<$ 1 μa	
beam voltage	25 kV Infodex, 12 kV APS-94	
maximum spatial frequency to be handled in range	31.5 ℓp/mm	Table 6.1
desired spot size across entire trace	16.3 μm (0.64 mils)	Table 6.1
beam velocity	6.66×10^5 mm/s	
LENS		
f-number	$\leq$f/4.0	
MTF	$\geq$50% at 43 ℓp/mm at image	Table 6.1
magnification, M	1/1.36 = 0.735	
object field	4.25 inches (108 mm)	
image field	3.13 inches (79.4 mm)	
FILM PLANE		
trace length	79.4 mm	
nominal trace velocity	4.90×10^5 mm/s	
nominal film velocity	40 mm/s	
maximum spatial frequency to be handled in range	42.9 ℓp/mm	Table 6.1
desired spot size across entire trace	12.0 μm	
minimum exposure available: Infodex	0.09 ergs/cm^2	Table 9.1
APS-94D	0.04 ergs/cm^2	Table 9.1
change of positional error of sweep (combined error of CRT and distortion of lens) measured at film plane	$<$5.8 μm over any 16.6 mm interval	Section 8.1
maximum deviation of beam velocity from average velocity relative to av. velocity	$\leq$ 0.04%	Section 8.1
maximum deviation of film velocity from average velocity relative to av. velocity		
a) 6.5 m resolution	$\leq$ 0.02%	
b) 25 m resolution, 1 look	$\leq$ 0.35%	Table 8.1

14. REFERENCES

1. Kozma, A., E.N. Leith, and N.G. Massey, *Tilted-plane Optical Processor*, Appl. Opt., Vol. 11, pp. 1766-1777, August 1972.

2. Liskow, C.L., et al., *Simultaneous Dual-band Radar Development*, Environmental Research Institute of Michigan, Radar and Optics Division, September 1974. NASA Report NASA CR-ERIM 195100-1-F.

3. Tsukkerman, I.I., *Electron Optics in Television*, Pergamon Press, Oxford 1961.

4. Bousky, S., and L. Teeple, *Laser Recording Performance with Spatial Error Compensation*, in Laser Recording, Proc. Soc. Photo-Opt. Inst. Eng. (S.P.I.E.), Vol. 53, August 1974, pp. 133-139.

5. Jablonowski, D.P., and J. Raamot, *Galvanometer Deflection: A Precision High-speed System*, Appl. Opt., pp. 1437-1443, June 1976.

6. Felstead, E.B., *System-design Considerations for an Optical Correlator for the Canadian Portion of the SEASAT-A SAR*, to be published as a CRC Report.

7. Born, M., and E. Wolf, *Principles of Optics*, 3rd ed. Pergamon Press, Oxford, 1965.

8. Bondurant, R.A., and K.G. Lieb, *Birefringence Effects in Estar Base Reconnaissance Film in an Optical Correlator*, Optics and Laser Technology, pp. 124-128, June 1977.